

## MeV sterile neutrinos in low reheating temperature cosmological scenarios

Graciela Gelmini<sup>1,2</sup>, Efunwande Osoba<sup>1</sup>, Sergio Palomares-Ruiz<sup>3</sup> and Silvia Pascoli<sup>3</sup>

<sup>1</sup> *Department of Physics and Astronomy, UCLA, Los Angeles, CA 90095, USA*

<sup>2</sup> *CERN PH-TH, CH-1211, Geneva 23, Switzerland*

<sup>3</sup> *IPPP, Department of Physics, Durham University, Durham DH1 3LE, UK*

It is commonly assumed that the cosmological and astrophysical bounds on the mixings of sterile with active neutrinos are much more stringent than those obtained from laboratory measurements. We point out that in scenarios with a very low reheating temperature  $T_{\text{RH}} \ll 100$  MeV at the end of (the last episode of) inflation or entropy creation, the abundance of sterile neutrinos becomes largely suppressed with respect to that obtained within the standard framework. Thus, in this case cosmological bounds become much less stringent than usually assumed, allowing sterile neutrinos to be “visible” in future experiments. Here, we concentrate on massive (mostly sterile) neutrinos heavier than 1 MeV.

PACS numbers: 14.60.St, 98.80.Cq

### I. INTRODUCTION

In inflationary models, the beginning of the radiation dominated era of the Universe results from the decay of coherent oscillations of a scalar field and the subsequent thermalization of the decay products into a thermal bath with the so called “reheating temperature”,  $T_{\text{RH}}$ . The standard computation of the relic densities relies on the assumptions that  $T_{\text{RH}}$  was large enough for the particles of interest to have reached thermal equilibrium and that the entropy of matter and radiation is conserved after they decouple. However, there are non-standard cosmological models in which these assumptions about the epoch of the Universe before Big Bang Nucleosynthesis (BBN), an epoch from which we have no data, do not hold. These include models with moduli decay [1], Q-ball decay [2], and thermal inflation [3]. In all of these models there is a late episode of entropy production in which the Universe is reheated to a low  $T_{\text{RH}}$ . This temperature may have been as low as  $\sim 4$  MeV [4] once all cosmological data are taken into account, while BBN-only data impose a lower bound of  $\sim 2$  MeV on  $T_{\text{RH}}$  [5] if active neutrino oscillations are taken into account (up from  $\sim 0.7$  MeV [6] if they are not). It is well known that a low reheating temperature inhibits the production of particles which are non-relativistic or decoupled at  $T \lesssim T_{\text{RH}}$  [7, 8, 9]. The final number density of active neutrinos starts departing from the standard number for  $T_{\text{RH}} \lesssim 8$  MeV but stays within 10%, 20% or 50% of it for  $T_{\text{RH}} \gtrsim 5$  MeV, 4 MeV and 3 MeV, respectively. For  $T_{\text{RH}} = 1$  MeV the number of tau- and muon-neutrinos would be about 2.7% of the standard number [8, 10].

Low  $T_{\text{RH}}$  cosmological scenarios are more complicated than the standard ones. Different aspects of these models have been studied with interesting results, but no consistent all-encompassing scenario exists yet. Baryogenesis could be produced through the Affleck-Dine mechanism, in a model similar to that of Ref. [11]. Dark matter could still consist of the lightest supersymmetric particle or other Weakly Interactive Massive Particles (WIMPs), produced either thermally or non-thermally [12]. Alternatively, MeV scalars have been proposed as DM candidates [13, 14]: they would be in thermal equilibrium in the Early Universe with neutrinos, electrons, positrons and photons and would freeze-out at 100’s keV– MeV temperatures.

If sterile neutrinos exist and have no extra standard-model interactions, the dominant mechanism of production in the early Universe is through their mixing with active neutrinos [15]. Dodelson and Widrow [16] (see also Refs. [17, 18]) provided the first analytical calculation of the production of sterile neutrinos lighter than 100 keV in the early Universe, under the assumption (which we maintain here) of a negligible primordial lepton asymmetry.

In general, given that the production rate of sterile neutrinos of mass  $m_s$  is maximum at a temperature  $T_{\text{max}} \simeq 1.3$  GeV  $(m_s/\text{MeV})^{1/3}$  [15, 16], if the reheating temperature is smaller,  $T_{\text{RH}} < T_{\text{max}}$ , the production of sterile neutrinos is suppressed. Hence, the main idea of this paper is that the primordial abundance of sterile neutrinos does not necessarily impose their mixing with active neutrinos to be small. A low reheating temperature scenario would suppress the sterile neutrino production, weakening the cosmological bounds. Thus, it might be possible to consider massive (mostly sterile) neutrinos of any mass and mixing with active ones, as long as laboratory bounds are satisfied. These neutrinos could, therefore, be revealed in future experiments. We concentrate here on the production of massive (mostly sterile) neutrinos heavier than 1 MeV through the conversion of active neutrinos for  $T_{\text{RH}} < m_s$ ,

having already applied the same ideas to lighter sterile neutrinos [9]. By using different approximations, we obtain an analytical result for the sterile neutrino abundance. In this way, we are able to write all our results in a simplified form. Although it is a rough approximation, it allows us to have a qualitative understanding of the problem. For lighter neutrinos,  $m_s < 1$  MeV, the analytical calculation of Ref. [9] of the final sterile neutrino abundance turned out to be correct within an order of magnitude [10]. Like in Ref. [9], here the active neutrinos are assumed to have the usual thermal equilibrium distribution  $f_A = (\exp(E/T) + 1)^{-1}$  with  $E = p$ . Thus, following Ref. [4], we restrict ourselves to reheating temperatures  $T_{\text{RH}} > 4$  MeV.

The paper is organized as follows. In Section II we obtain an analytical approximation for the sterile neutrino abundance as a function of the reheating temperature. In Section III we describe the laboratory bounds for sterile-active neutrino mixing for each of the three active flavors. Using the result of Section II, we compute in Section IV the astrophysical and cosmological bounds and show how, in some cases, they are completely evaded. Finally, in Section V, we draw our conclusions.

## II. STERILE NEUTRINO ABUNDANCE

For simplicity, our analysis is based on the two-neutrino mixing approximation. In this way, an analytical understanding of the problem is possible. Within this approximation, the vacuum mixing angle  $\sin\theta$  represents the amplitude of the heavy mass eigenstate  $\nu_2$  in the composition of the active neutrino flavor eigenstate  $\nu_\alpha$ , i.e.,  $\nu_\alpha = \cos\theta \nu_1 + \sin\theta \nu_2$ ,  $\nu_s = -\sin\theta \nu_1 + \cos\theta \nu_2$  for  $\alpha = e, \mu, \tau$ , where  $\nu_1$  is the light mass eigenstate and  $\nu_2$  is the heavy mass eigenstate, which for small  $\sin\theta$  is mostly sterile and whose mass we call  $m_s$ .

In order to obtain the distribution function of sterile neutrinos at a given temperature after the last episode of inflation, we start from the Boltzmann equation<sup>1</sup>,

$$\left( \frac{\partial}{\partial t} - H p \frac{\partial}{\partial p} \right) f_s = I_{\text{coll}} , \quad (2.1)$$

where  $I_{\text{coll}} \simeq \Gamma_s(T) (f_s^{\text{eq}} - f_s)$  is the collision integral. Here,  $f_s^{\text{eq}} = (\exp(E/T) + 1)^{-1}$  is the Fermi-Dirac distribution that heavy neutrinos would have if they were in thermal equilibrium. In many cases the approximation  $T \propto 1/a$ , with  $a$  the scale factor, is sufficiently accurate. Hence, by using  $\dot{T} = -HT$ , Eq. (2.1) can be rewritten as (see e.g. Ref. [20]),

$$-HT \left( \frac{\partial f_s}{\partial T} \right)_{p/T} \simeq \Gamma_s(T) (f_s^{\text{eq}} - f_s) . \quad (2.2)$$

For neutrino masses much smaller than the temperature of the plasma,  $\langle p \rangle \simeq \langle E \rangle$ , ( $m_s < 1$  MeV), the averaged rate of sterile neutrino interactions is given by

$$\Gamma_s(T) \simeq \frac{1}{4} \sin^2 2\theta_m d_\alpha G_F^2 E T^4 , \quad (2.3)$$

where  $\theta_m$  is the mixing angle in matter,  $G_F$  is the Fermi constant and  $d_\alpha = 1.13$  for sterile neutrino mixing with  $\nu_\alpha = \nu_e$  and  $d_\alpha = 0.79$  with  $\nu_\alpha = \nu_{\mu, \tau}$ . For  $T < 1.5$  GeV ( $m_s/\text{MeV}$ )<sup>1/3</sup> matter effects are negligible [19] and hence  $\sin^2 2\theta_m \simeq \sin^2 2\theta$  is a very good approximation. Plugging Eq. (2.3) into Eq. (2.2), and solving for  $f_s$  in the limit  $f_s \ll f_s^{\text{eq}}$ , the distribution function of massive (mostly sterile) neutrinos lighter than 1 MeV was found to be [9]

$$f_s(E, T) \simeq 3.2 d_\alpha \left( \frac{T_{\text{RH}}}{5 \text{ MeV}} \right)^3 \sin^2 2\theta \left( \frac{E}{T} \right) f_s^{\text{eq}} , \quad (2.4)$$

for  $T_{\text{RH}} \ll T_{\text{max}}$ . This distribution results in a number density of light ( $m_s < 1$  MeV) sterile neutrinos given by

$$n_s \simeq 10 d_\alpha \sin^2 2\theta \left( \frac{T_{\text{RH}}}{5 \text{ MeV}} \right)^3 n_\alpha , \quad (2.5)$$

where  $n_\alpha = 0.09 g T^3$  is the number density of a relativistic fermion with  $g$  degrees of freedom in thermal equilibrium. Notice that the number density of sterile neutrinos depends on both the active-sterile mixing angle and the reheating

---

<sup>1</sup> The distribution functions are defined for mass eigenstates (see the Appendix).

temperature. A low reheating temperature implies a small sterile number density, even for active-sterile mixing angles as large as experimental bounds permit (see below). However, Eq. (2.4) is only valid if the condition  $f_s \ll f_s^{\text{eq}}$  is satisfied. We would like to extend here this result, for the case when this approximation starts to fail. This was not included in Ref. [9]. Nevertheless, Eq. (2.2) can be solved perturbatively and Eq. (2.4) should be replaced by

$$f_s(E, T) \simeq (1 - e^{-S}) f_s^{\text{eq}}(E, T) , \quad (2.6)$$

where  $S = 3.2 d_\alpha (T_R/5 \text{ MeV})^3 (E/T) \sin^2 2\theta$  is the coefficient multiplying the equilibrium neutrino distribution in Eq. (2.4). The sterile neutrino number density  $n_s$  results from a numerical integration of this distribution. This perturbative solution is valid for  $S < 1$ .

For heavier sterile neutrinos, with  $m_s > 1 \text{ MeV}$ , and for the range of temperatures explored here, the heavy neutrino mass needs to be taken into account and the averaged production rate of sterile neutrinos  $\Gamma_s$  is given by [19, 20]

$$\Gamma_s(T) = \frac{1}{\tau_s} \left[ \frac{m_s}{E} + \frac{3 \times 2^7 T^3}{m_s^3} \left\{ \frac{3 \zeta(3)}{4} + \frac{7 \pi^4}{144} \left( \frac{ET}{m_s^2} + \frac{p^2 T}{3 E m_s^2} \right) \right\} \right] , \quad (2.7)$$

where the first term is due to inverse decay and the other terms correspond to two-to-two particle processes. The last term in parenthesis,  $\sim T^4/\tau_s m_s^5$ , due to oscillations, is the only one remaining as  $m_s \rightarrow 0$ <sup>2</sup>. The function  $\tau_s$  in the denominator is the heavy neutrino lifetime. As in the case of  $m_s < 1 \text{ MeV}$ , Eq. (2.7) is valid when matter effects are not important.

For  $m_s < m_\pi \sim 140 \text{ MeV}$ , the massive (mostly sterile) neutrino can decay into a light neutrino and two leptons  $\nu_s \rightarrow \nu_\alpha + l + \bar{l}$ , mainly  $\nu_\alpha \bar{\nu} \nu$  and  $\nu_\alpha e^+ e^-$ . If the active neutrino mixing with the sterile is  $\nu_\tau$  or  $\nu_\mu$ , the decay of  $\nu_2$  happens through neutral currents and the lifetime is

$$\tau_s = \frac{1.0 \text{ sec}}{\sin^2 2\theta} \left( \frac{10 \text{ MeV}}{m_s} \right)^5 . \quad (2.8)$$

If instead  $\nu_s$  mixes mostly with  $\nu_e$ , the factor 1.0 sec should be replaced by 0.7 sec [19, 20], due to the presence of charged currents. However, we are not going to keep this distinction in the following. For  $m_\pi < m_2 < 2m_\mu$ ,  $\nu_2$  decays mostly into  $\pi^0 \nu$ ,  $\pi^+ e^-$  and  $\pi^- e^+$ , and the decay is much faster than Eq. (2.8) [19, 21]. For even larger masses, other decay modes open up. In the following we will restrict ourselves to the range  $m_s < m_\pi \simeq 140 \text{ MeV}$ , which is enough for our purposes of showing the main characteristics of the low reheating temperature cosmological scenarios we envision.

Assuming that the bulk of sterile neutrinos are produced after the reheating of the Universe<sup>3</sup>, namely that  $f_s \simeq 0$  at  $T = T_{\text{RH}}$ , we solve analytically Eq. (2.2) for  $T_{\text{RH}} \leq m_s$ , after plugging Eqs. (2.7) and (2.8) into it. In order to analytically solve the equation, we will make several approximations. First, we assume that the actual distribution function of the heavy neutrinos is always much smaller than the equilibrium distribution,  $f_s \ll f_s^{\text{eq}}$ . Then, we approximate the Fermi-Dirac distribution by a Boltzmann distribution,  $f_s^{\text{eq}} \simeq e^{-E/T}$  and take neutrinos to be either purely non-relativistic, i.e.,  $E_2 = m_s$  if  $p_2 < m_s$ , or purely relativistic, i.e.,  $E_2 = p_2$  if  $p_2 > m_s$ . We define  $y \equiv p/T$ , and integrate analytically Eq. (2.2) (with  $y$  constant) over temperatures  $T$  in the interval  $0 \leq T \leq T_{\text{RH}}$ . We find  $f_I$  and  $f_{II}$  given by

$$f_I(T, y) = \int_{m_s/y}^{T_{\text{RH}}} \frac{\Gamma_s(T)}{HT} e^{-y} dT + \int_0^{m_s/y} \frac{\Gamma_s(T)}{HT} e^{-m_s/T} dT , \quad (2.9)$$

for  $0 \leq m_s/y \leq T_{\text{RH}}$  and

$$f_{II}(T, y) = \int_0^{T_{\text{RH}}} \frac{\Gamma_s(T)}{HT} e^{-m_s/T} dT , \quad (2.10)$$

for  $T \leq T_{\text{RH}} \leq m_s/y$ . Notice that due to the Boltzmann factor the contribution of the integrands at low temperatures is negligible. Thus, cutting the integrations at the decoupling temperature of active neutrinos or extending them to zero temperatures does not change the integrals in any significant way.

<sup>2</sup> We note that in this limit there is a factor of 2 with respect to Eq. (2.3) already present in the previous literature, which does not change our conclusions and we do not attempt to correct here.

<sup>3</sup> It was shown in Ref. [10] that for masses lighter than 1 MeV this gives results which are correct within an order of magnitude [9].

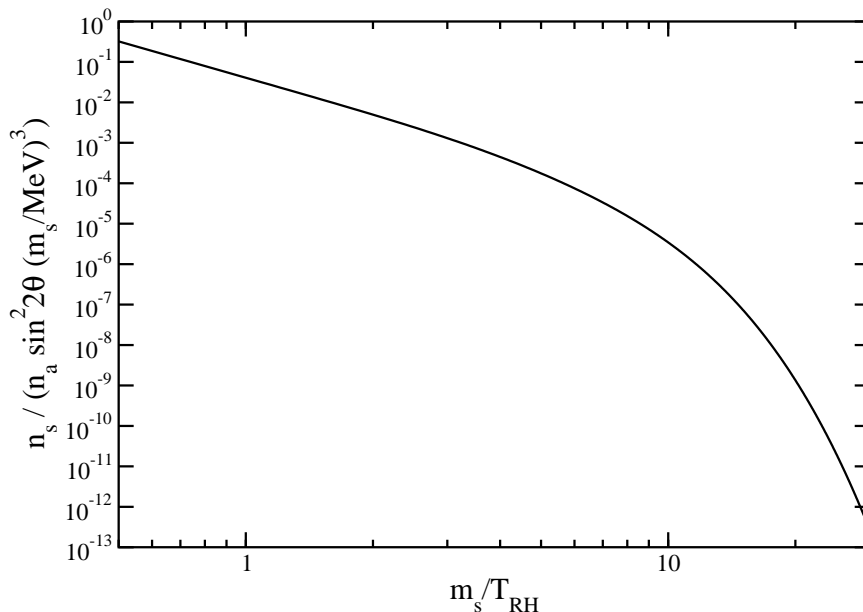


FIG. 1: Number density of (mostly) sterile neutrinos for  $1 \text{ MeV} < m_s < 140 \text{ MeV}$  and  $5 \text{ MeV} \leq T_{\text{RH}} \leq m_s$ .

Once we have the distribution function, we then find the sterile neutrino number density as function of the ratio  $m_s/T_{\text{RH}}$  and the temperature  $T$ , by integrating  $f_I$  and  $f_{II}$ ,

$$n_s(m_s/T_{\text{RH}}, T) = \int_0^{T(m_s/T_{\text{RH}})} \frac{p^2 dp}{2\pi^2} f_{II}(p, T) + \int_{T(m_s/T_{\text{RH}})}^{\infty} \frac{p^2 dp}{2\pi^2} f_I(p, T). \quad (2.11)$$

This procedure overestimates the final abundance, thus providing an upper bound on the actual abundance. In this way we find that the number density  $n_s$  of heavy (mostly sterile) neutrinos for  $m_s < 140 \text{ MeV}$  is given by

$$\begin{aligned} n_s(x_{\text{RH}}, T) &\simeq n_\alpha(T) \sin^2 2\theta \left(\frac{m_s}{\text{MeV}}\right)^3 2.1 \times 10^{-3} e^{-x_{\text{RH}}} \\ &\times \left[ \left(\frac{7}{3} + \frac{6 + 144\zeta(3)}{\pi^4}\right) + \frac{2^3 \times 7}{3} \left\{ 1 + x_{\text{RH}} + \left(\frac{3}{2^3} + \frac{3^4\zeta(3)}{7\pi^4}\right) x_{\text{RH}}^2 \right\} \frac{1}{x_{\text{RH}}^3} \right. \\ &\left. + \left( 24 + 144\zeta(3) + 12x_{\text{RH}} + \frac{7}{2}x_{\text{RH}}^2 + \frac{1}{2}x_{\text{RH}}^3 \right) \frac{x_{\text{RH}}}{4\pi^4} \right]. \end{aligned} \quad (2.12)$$

Here we have defined  $x_{\text{RH}} \equiv m_s/T_{\text{RH}}$ . This number density is plotted in Fig. 1, where  $n_s/[n_\alpha \sin^2 2\theta (m_s/\text{MeV})^3]$  is shown as function of  $x_{\text{RH}}$ . Taking into account the subsequent decay of sterile neutrinos, the actual number density is  $n_s(T) \simeq n_s(x_{\text{RH}}, T) e^{-t/\tau_s}$ . In order to obtain analytical results for the cosmologically and astrophysically allowed regions in the parameter space  $(\sin^2 2\theta, m_s)$ , in Section IV we will use the instant-decay approximation for  $\tau_s$  smaller than the age of the Universe.

We consider next the experimental bounds and then the cosmological and astrophysical bounds on the mass and mixing angle of heavy (mostly sterile) neutrinos. We will show that if the reheating temperature turns out to be sufficiently smaller than the neutrino mass, the cosmological bounds become irrelevant and the mixing angles for any given mass can be as large as the experimental bounds permit, making the detection at the reach of future laboratory experiments.

### III. EXPERIMENTAL BOUNDS

In laboratory searches, no positive evidence of heavy (mostly sterile) neutrinos has been found so far in the mass range of interest, 1 MeV–140 MeV. Here, we review the most stringent bounds on the mixing angle with active neutrinos and show them in Figs. 2 and 3 (for further details see a comprehensive discussion in Ref. [22]).

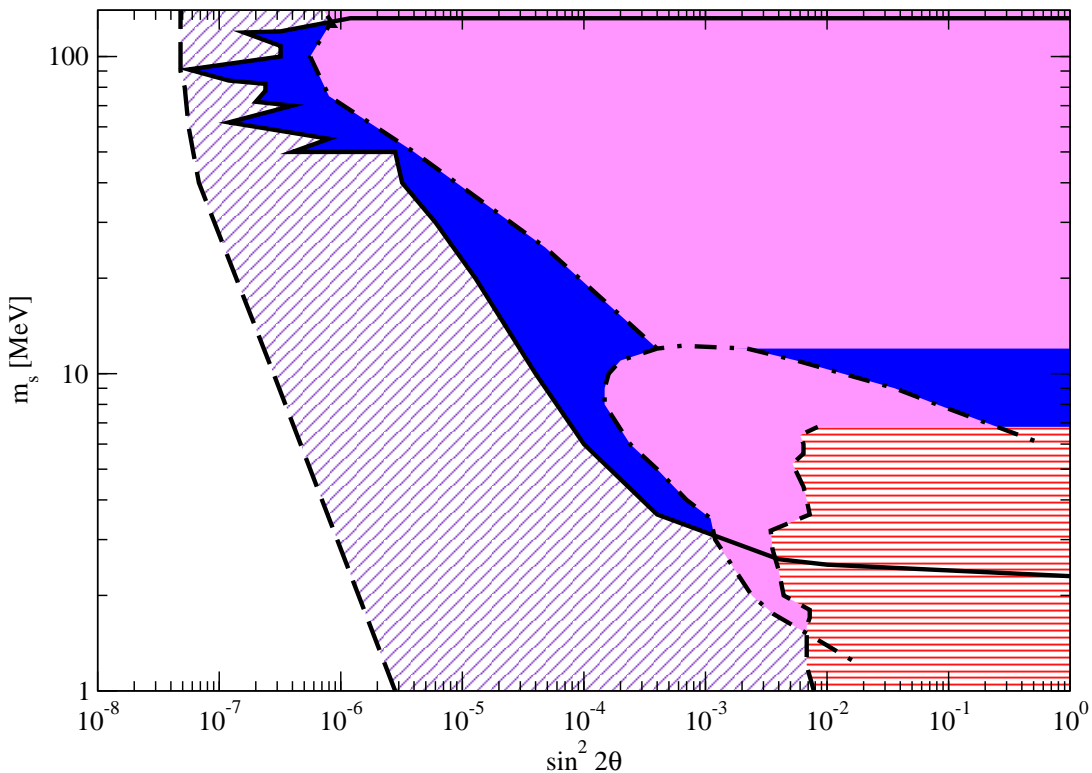
$\nu_e - \nu_s$  mixing


FIG. 2: Experimental bounds on the mass and mixing angle of sterile neutrinos mixed with  $\nu_e$  in the mass range  $1 \text{ MeV} < m_s < 140 \text{ MeV}$ . The colored regions are excluded by searches of: i) kinks in  $\beta$ -decays: horizontally hatched (red) area with short-dashed boundary; ii) sterile neutrino decays in visible particles: solid light gray (magenta) regions with dash-dotted contours; iii) peaks in the electron spectrum in pion and kaon decays: solid dark gray (blue) region delimited by a solid line; iv) neutrinoless double beta-decay: diagonally hatched (blue) area with long-dashed contour. See text for details.

Let us consider first sterile neutrinos mixing with  $\nu_e$ . For masses up to  $m_s \simeq 10 \text{ MeV}$ , an important bound is provided by searches of kinks in the electron spectrum of  $\beta$ -decays, which constrain the mixing angle to be  $\sin^2 2\theta \lesssim 6 \times 10^{-3}$ , as shown in the horizontally hatched (red) excluded region in Fig. 2.

For higher masses, very robust bounds can be set by looking for additional peaks in the spectrum of electrons in leptonic decays of pions and kaons. The electron energy of the possible monochromatic line, given by  $E_l = (m_{\pi,K} + m_e^2 - m_s^2)/2m_{\pi,K}$ , depends on the mass of the heavy sterile neutrino, while the branching ratio is proportional to  $\sin^2 2\theta$ . Here,  $m_{\pi,K}$  is the mass of either the pion or the kaon respectively,  $m_e$  is the mass of the electron and  $m_s$  is the sterile neutrino mass. At present, bounds as stringent as  $\sin^2 2\theta < 10^{-7}$  are obtained in this way (for a review see Ref. [23]) which are shown in Fig. 2 as the solid dark gray (blue) excluded area.

In neutrino-oscillation, fixed-target and collider experiments, if sterile neutrinos mix with active ones, a beam of  $\nu_s$  would be produced and would subsequently decay into visible particles. Assuming only charged current and neutral current interactions for  $\nu_s$ , the absence of  $\nu_s$ -decay signatures in past and present experiments allows one to put limits on the mixing term which controls the intensity of the  $\nu_s$  beam and the decay time. A reanalysis of the Borexino Counting Test Facility and Bugey data yields  $\sin^2 2\theta < 10^{-4}$  for  $m_s < 10 \text{ MeV}$  [24] at 90% confidence level (CL), while the data from the experiment PS191 [25] puts a bound which is strongly mass dependent, going from  $\sin^2 2\theta < 4 \times 10^{-4}$  at  $m_s \sim 12 \text{ MeV}$  to  $\sin^2 2\theta < 10^{-8}$  at  $m_s \sim 300 \text{ MeV}$ . These constraints exclude the solid light gray (light-magenta) regions in Fig. 2.

Finally, if sterile neutrinos are Majorana particles, they would contribute to the mediation of neutrinoless double beta decay. The limit on the half-life time of this process can be translated into a bound on the mixing with  $\nu_e$ ,  $\sin^2 \theta$ , which scales as  $m_s$  for  $m_s \lesssim 30 \text{ MeV}$  and as  $m_s^{-1}$  for  $m_s \gtrsim 400 \text{ MeV}$ , with  $\sin^2 2\theta < 5 \times 10^{-8}$  at  $m_s \sim 100 \text{ MeV}$ . This limit excludes the diagonally hatched (blue) region shown in Fig. 2.

Let us now consider the case of mixing with  $\nu_\mu$ . As discussed above for the case of sterile neutrinos mixing with

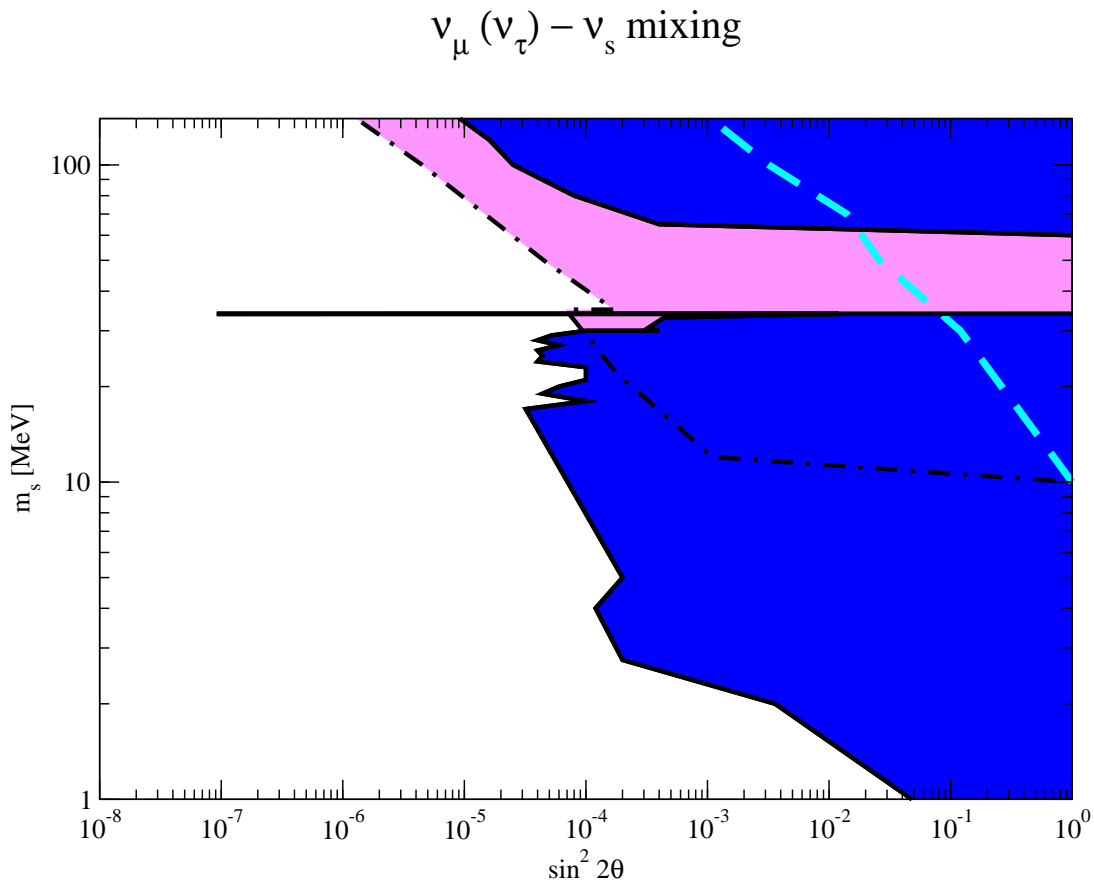


FIG. 3: Experimental bounds on the mass and mixing angle of sterile neutrinos mixed with  $\nu_\mu$  (or with  $\nu_\tau$ ) in the mass range  $1 \text{ MeV} < m_s < 140 \text{ MeV}$ . For the  $\nu_\mu$  case, the colored regions denote the bounds obtained from i) peak searches in the muon spectrum from pion and kaon decays which exclude the dark gray (blue) areas with solid contours; ii) searches of sterile neutrino decays excluding the light gray (light-magenta) region delimited by a dash-dotted line. The (cyan) long-dashed line represents the upper bound for sterile neutrinos mixed with  $\nu_\tau$ . See text for further details.

$\nu_e$ , peak searches provide very robust and stringent bounds on sterile neutrinos. Looking this time for peaks in the spectrum of muons in pion decays, it is possible to constrain the relevant mixing  $\sin^2 2\theta$  to be typically  $< 10^{-4}$  in the mass range 4–34 MeV (for a detailed review see Fig. 1 of Ref. [26]). Motivated by the KARMEN anomaly, which could be explained by the existence of a heavy (mostly sterile) neutrino with mass 33.9 MeV, very sensitive searches have been performed for this neutrino mass and the bound was found  $\sin^2 2\theta < 9.2 \times 10^{-8}$  at 95% CL [27] (see the black horizontal line in Fig. 3). Similarly, sterile neutrinos with heavier masses can be probed in kaon decays and, in the mass range of interest, the derived bounds go from  $\sin^2 2\theta < 4 \times 10^{-4}$  at  $m_s = 65 \text{ MeV}$  to  $\sin^2 2\theta < 25.2 (4) \times 10^{-6}$  for  $m_s = 100 \text{ MeV}$  (200 MeV) at 90% CL [28]. These peak-searches exclude the dark gray (blue) areas shown in Fig. 3.

By searching for the production of  $\nu_s$  in pion and kaon decays and their subsequent decay, a reanalysis [26] of fixed-target data led to a stringent mass-dependent bound on  $\sin^2 2\theta$ , which exclude the light gray (light-magenta) area in Fig. 3. The bound is  $\sin^2 2\theta < 10^{-4}$  for masses up to 35 MeV and reaches  $\sin^2 2\theta < 3.4 \times 10^{-7}$  at  $m_s = 200 \text{ MeV}$ , at 90% CL. Similar bounds can be set on the product of the mixing angle with  $\nu_\mu$  and with  $\nu_e$  from the analysis of the same decay-searches data (a review is given in Ref. [26]).

Let us consider finally the case of heavy (mostly sterile) neutrinos mixed with  $\nu_\tau$ . The only limits on these sterile neutrinos come from searches for  $\nu_s$  decays. The most stringent bound is obtained by the reanalysis of data from the CHARM experiment, in which  $\nu_s$  could be produced in  $D$  and  $\tau$  decays. However, in the mass range we are considering, this upper bound, shown in Fig. 3 by the (red) long-dashed line, is rather weak, such as  $\sin^2 2\theta < 2 \times 10^{-3}$  for  $m_s = 100 \text{ MeV}$ .

#### IV. COSMOLOGICAL BOUNDS

In what follows we obtain four different types of cosmological and astrophysical bounds on the parameter space of active-sterile neutrino mixing,  $(\sin^2 2\theta, m_s)$ . Each of these limits is valid for a certain range of values of the heavy neutrino lifetime,  $\tau_s$ . Whereas the first three bounds we describe have to do with the photons which are produced in the decay, the last one represents a bound on the sterile neutrino abundance at a particular epoch. Finally, we will also comment on bounds from core collapse supernovae observations.

In the first place, we consider the diffuse extragalactic background radiation (DEBRA) spectrum and set bounds on the basis of not finding any unexpected result from heavy (mostly sterile) neutrino decay. Secondly, we obtain bounds using the non-observation of a distortion of the Cosmic Microwave Background (CMB) spectrum caused by the radiation from decay. Then, we calculate the limits based on the data from the primordial light element abundances and how neutrino decay would affect them. Finally, we also use the upper bound from BBN on the extra number of relativistic degrees of freedom at that epoch to set a limit on active-sterile neutrino mixing. In our analysis, for  $\tau_s < t_U$  with  $t_U \simeq 14$  Gyr the present age of the Universe, we use the instant-decay approximation, i.e., all decays happen at  $t = \tau_s$ . This will allow us to obtain all the results analytically, while giving rise to accurate enough calculations for our purposes.

For sterile neutrino masses in the range of interest,  $1 \text{ MeV} < m_s < 140 \text{ MeV}$ , the decay branching ratio of  $\nu_2$  into  $e^+e^-$  is about 10% (40%) for mixing with  $\nu_\mu$  or  $\nu_\tau$  ( $\nu_e$ ). Due to inverse Compton scattering on the CMB with a Thompson cross section, the interaction length of these electrons is about 1 kpc (see for example Ref. [29] or Fig. 5 of Ref. [30]) and the result of each of the interactions is a photon that shares a large portion of the incoming electron energy. Photons at these energies propagate for cosmological distances undisturbed by the CMB or infrared backgrounds and are subjected to different cosmological bounds, which depend on the time at which the photons were produced.

Photons decouple from the plasma filling the Universe at the recombination epoch,  $t_{\text{rec}} \simeq 1.3 \times 10^{13}$  sec. Thus, if the sterile neutrino decays happen after recombination,  $\tau_s > t_{\text{rec}}$ , the photons produced do not interact ever after and could leave an imprint in the DEBRA spectrum [31]. Such a signature has not been observed, and thus the photon flux must not be larger than the observed DEBRA energy flux  $I_\gamma \equiv E_\gamma^2 dF_\gamma/dE_\gamma$ . From the observations by the COMPTEL [32] instrument we obtain approximately

$$I_\gamma \simeq 0.01 \frac{\text{MeV}}{\text{cm}^2 \text{ sec sr}} , \quad (4.1)$$

for  $1 \text{ MeV} < f_\gamma m_s < 30 \text{ MeV}$ , where  $f_\gamma$  is the average fraction of the sterile neutrino mass that goes into photons in each decay. Thus  $f_\gamma m_s$  is the average energy going into photons per decay. From EGRET data [31] we obtain

$$I_\gamma \simeq 2.0 \times 10^{-3} \frac{\text{MeV}}{\text{cm}^2 \text{ sec sr}} , \quad (4.2)$$

for  $30 \text{ MeV} < f_\gamma m_s < 140 \text{ MeV}$ . In the instant-decay approximation, for  $\tau_s < t_U$ , the energy of the photons produced in the decays at  $t = \tau_s$  redshifts from the time  $t = \tau_s$  until today. For  $\tau_s > t_U$ , because the decay rate increases with time for  $t < \tau_s$ , most of the decays are happening at present, and we assume there is no significant redshift of the initial photon energy. For  $\tau_s > t_U$ , we get

$$f_\gamma B m_s \frac{3}{2} \left( \frac{t_U}{\tau_s} \right) n_s \frac{c}{4\pi} < I_\gamma \quad (4.3)$$

and for  $t_{\text{rec}} < \tau_s < t_U$ ,

$$f_\gamma B m_s \left( \frac{\tau_s}{t_U} \right)^{2/3} n_s \frac{c}{4\pi} < I_\gamma , \quad (4.4)$$

where  $B$  is the branching ratio of the sterile neutrino decay into photons or charged particles. We label these bounds as ‘‘DEBRA’’ and it only appears in Fig. 7.

On the other hand, the CMB radiation is emitted at recombination. Electromagnetic decay products produced sometime before recombination may distort the CMB spectrum [33, 34]. Non-thermal photons produced before the thermalization time  $t_{\text{th}} \simeq 10^6$  sec are rapidly incorporated into the Planck spectrum. This happens through processes that change the number of photons, such as double Compton scattering ( $\gamma e \rightarrow \gamma \gamma e$ ). If non-thermal photons are produced after  $t_{\text{th}}$ , i.e., if  $t_{\text{th}} < \tau_s < t_{\text{rec}}$ , the CMB Planck spectrum would be distorted. Current data pose very stringent upper bounds on possible distortions of this spectrum. For the earliest part of this last time interval, i.e., for  $t_{\text{th}} \simeq 10^6 \text{ sec} < \tau_s < 10^9 \text{ sec}$ , photon number preserving processes, like elastic Compton scattering, are still efficient.

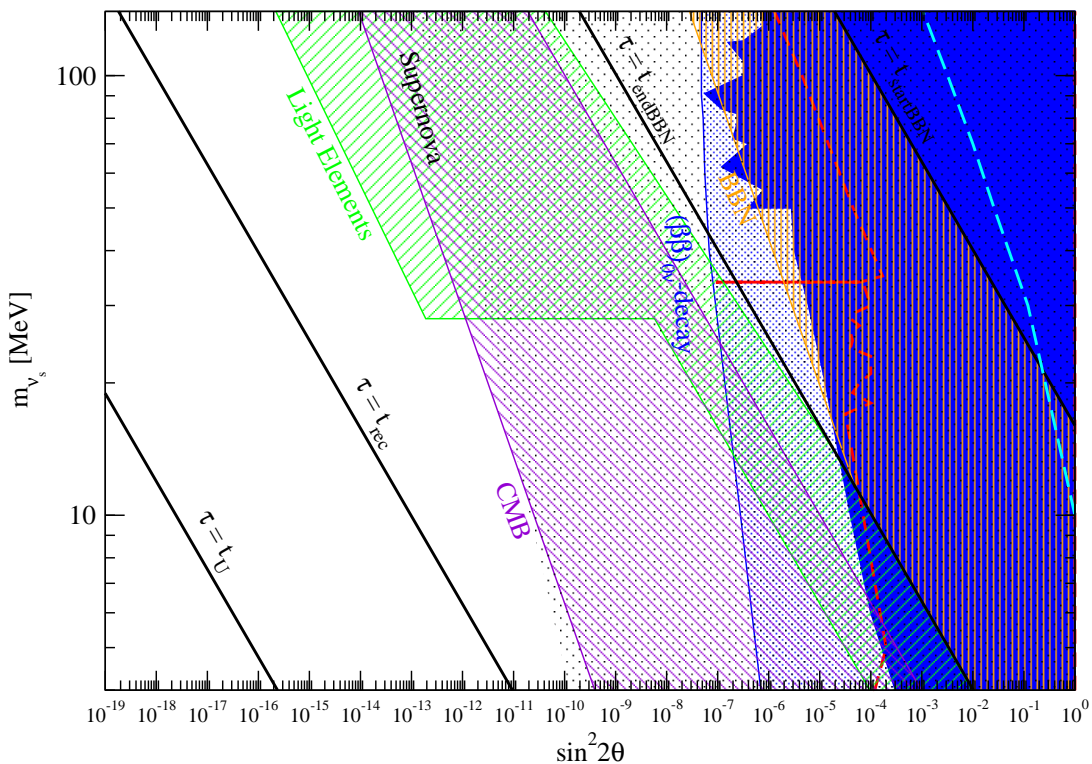


FIG. 4: Experimental and cosmological bounds as function of the mixing angle and mass of heavy (mostly sterile) neutrinos mixed with active ones for  $T_{\text{RH}} = m_s$ . The dark gray (blue) solid area and dark gray (blue) hatched area (for Majorana neutrinos) represent the experimentally excluded region for  $\nu_e - \nu_s$  mixing, the (red) short-dashed line and the (cyan) long-dashed line are the experimental upper bounds for  $\nu_\mu - \nu_s$  and  $\nu_\tau - \nu_s$  mixing, respectively. The cosmological and astrophysical bounds are indicated by the corresponding labels. Isolines for values of the heavy neutrino lifetime  $\tau$  equal to the start and end of the BBN epoch, the recombination time and the present age of the Universe are also shown. Only values of the reheating temperature larger than 4 MeV are considered. See text for details.

These processes thermalize the photons not into a Planck spectrum but into a Bose-Einstein spectrum with a non-zero chemical potential  $\mu$ . If the initial spectrum has fewer photons than a black body of the same total energy, then the chemical potential is positive  $\mu > 0$  (if it has more photons, then  $\mu < 0$ ). So, for  $t_{\text{th}} \simeq 10^6 \text{ sec} < \tau_s < 10^9 \text{ sec}$ , the energy released into photons in the decay for  $|\mu| \ll 1$  (the only values of  $\mu$  allowed by observations) is

$$\frac{\Delta\rho_\gamma}{\rho_\gamma} \simeq 0.714\mu. \quad (4.5)$$

The bound provided by the COBE satellite is  $|\mu| < 0.9 \times 10^{-4}$  at the 95% CL [35]. For later decays,  $10^9 \text{ sec} < \tau_s < t_{\text{rec}}$ , the photon number preserving processes can no longer establish a Bose-Einstein spectrum. The energy released in this case is not thermalized but simply heats the electrons. Through inverse-Compton scattering this produces a distorted spectrum characterized by a parameter  $y$ , which for  $|y| \ll 1$  is related to the energy released in non-thermal photons as

$$\frac{\Delta\rho_\gamma}{\rho_\gamma} \simeq 4y. \quad (4.6)$$

The COBE upper bound on this parameter is  $|y| < 1.5 \times 10^{-5}$  [35]. In both cases, Eqs. (4.5) and (4.6), the fractional increase in the photon energy density due to the decay of the sterile neutrinos can be written as

$$\frac{\Delta\rho_\gamma}{\rho_\gamma} \simeq f_\gamma B \frac{m_s n_s}{2.7 n_\gamma} \left(\frac{\tau_s}{\text{sec}}\right)^{1/2} \lesssim 6 \times 10^{-5}. \quad (4.7)$$

All these bounds just described related to distortions in the CMB spectrum are labeled as “CMB” in Figs. 4, 5 and 7.

For decays at earlier times, the best constraints on photons produced before the CMB thermalization epoch  $t_{\text{th}}$  come from BBN which finishes by  $t_{\text{endBBN}} \simeq 10^4 \text{ sec}$ . After  $t_{\text{endBBN}}$ , electromagnetic cascades can cause the photodissociation of D and  ${}^4\text{He}$ . For photons produced in the time interval  $10^4 \text{ sec} < \tau_s < 10^6 \text{ sec}$ , the photodissociation of D

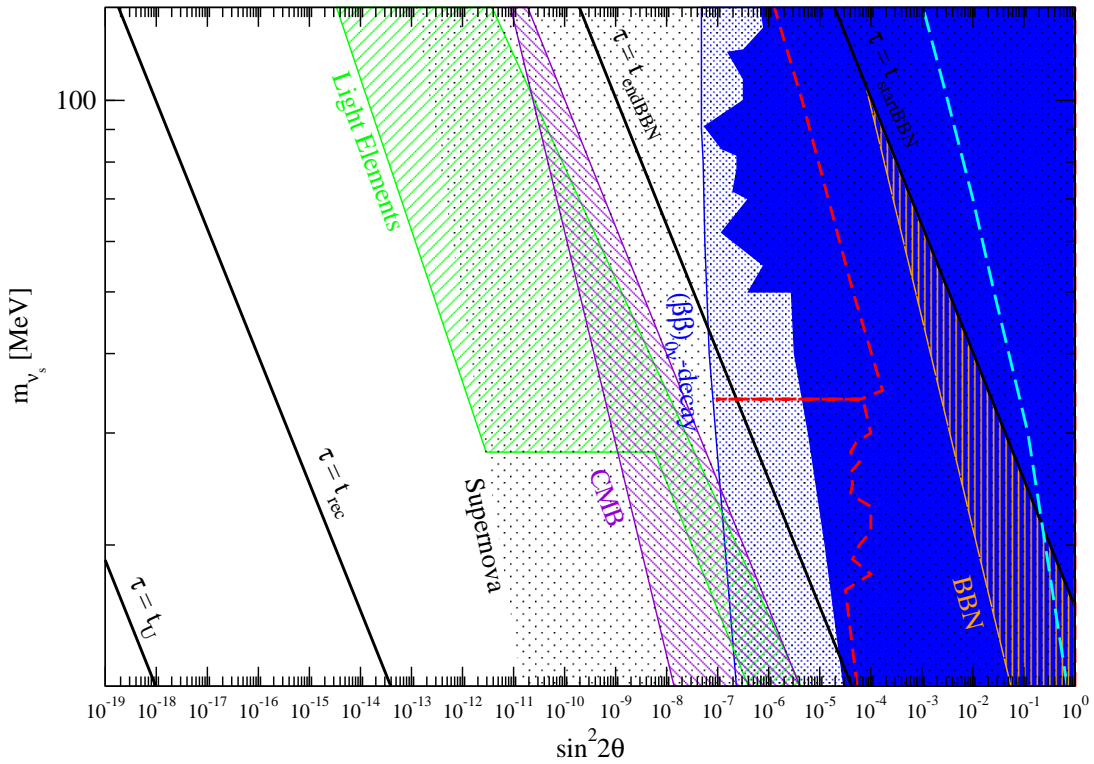


FIG. 5: Same as Fig. 4 but for  $T_{RH} = m_s/3$ .

poses the best limits. For earlier and later times, the overproduction of D due to the photodissociation of  ${}^4\text{He}$  [33] far dominates its destruction, since the abundance of  ${}^4\text{He}$  is about  $10^4$  times greater than that of D, and sets the most stringent constraints. The upper bounds taken from Fig. 3 of Ref. [33] are

$$\left(\frac{m_s}{\text{MeV}}\right) \frac{n_s}{n_\gamma} < 10^{-2} \left(\frac{10^4 \text{ sec}}{\tau_s}\right)^{5/2}, \quad (4.8)$$

for  $10^4 \text{ sec} < \tau_s < 10^6 \text{ sec}$  and  $m_s > 2.2 \text{ MeV}$ ;

$$\left(\frac{m_s}{\text{MeV}}\right) \left(\frac{n_s}{n_\gamma}\right) < 10^{-7} \left(\frac{10^6 \text{ sec}}{\tau_s}\right), \quad (4.9)$$

for  $10^6 \text{ sec} < \tau_s < 10^8 \text{ sec}$  and  $m_s > 28 \text{ MeV}$  and

$$\left(\frac{m_s}{\text{MeV}}\right) \left(\frac{n_s}{n_\gamma}\right) < 10^{-9} \left(\frac{\tau_s}{10^8 \text{ sec}}\right)^{1/4}, \quad (4.10)$$

for  $10^8 \text{ sec} < \tau_s < 10^{13} \text{ sec}$  and  $m_s > 28 \text{ MeV}$ . We label these bounds as “Light Elements” in Figs. 4, 5 and 7.

For even earlier times, BBN data provides an upper bound on any source of extra energy density present in the Universe during the BBN epoch,  $t_{\text{startBBN}} \simeq 0.1 \text{ sec} < \tau < t_{\text{endBBN}}$ , as well as on extra radiation present during that period. The bounds are complicated in detail, but it is safe to say that if the extra energy density due to the presence of sterile neutrinos is very small, BBN will not be affected in any way. The bounds on extra contributions to the energy density during BBN are customarily presented in terms of the equivalent extra number of relativistic active neutrino species  $\Delta N_\nu$ . Thus, to be on the safe side, we simply require the  $\Delta N_\nu$  due to the presence of sterile neutrinos to be very small during BBN:

$$\Delta N_\nu = \frac{\rho_s}{\rho_a} \simeq \frac{1}{\pi} \frac{n_s}{n_a} \left(\frac{m_s}{\text{MeV}}\right) \left(\frac{\tau}{\text{sec}}\right)^{1/2} < 1. \quad (4.11)$$

We label this bound as “BBN” in Figs. 4, 5 and 7.

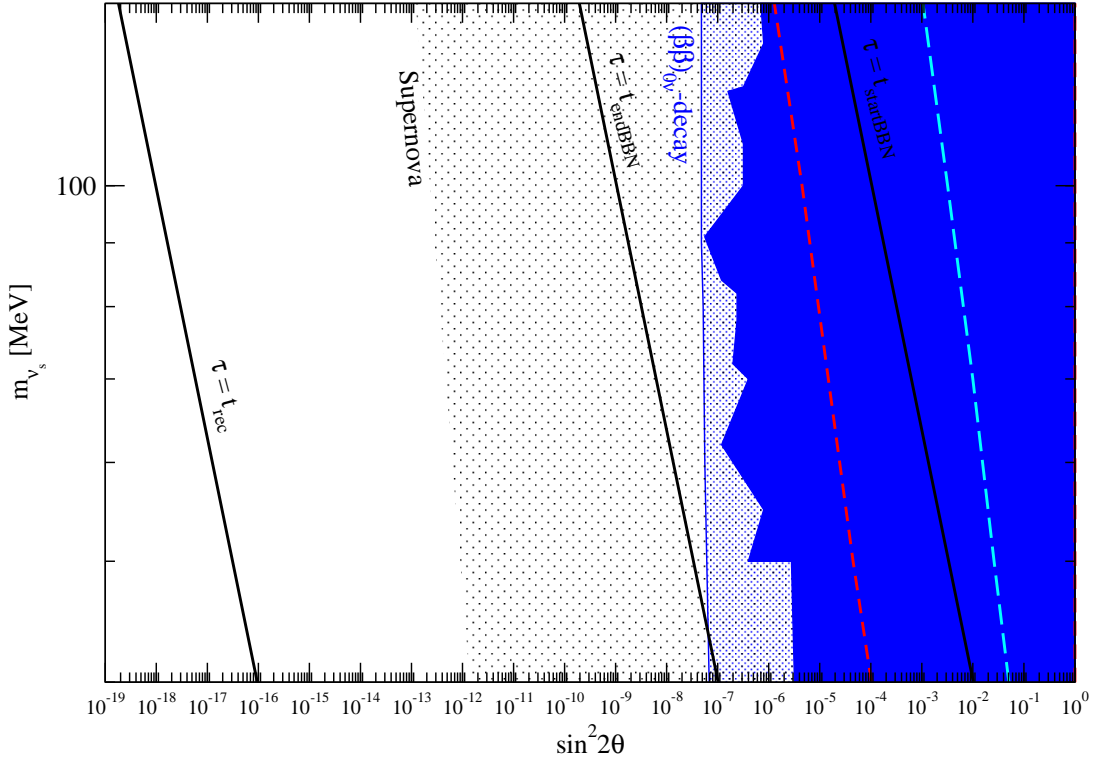


FIG. 6: Same as Fig. 4 but for  $T_{\text{RH}} = m_s/10$ .

Finally, there are also astrophysical disfavored regions in the  $(\sin^2 2\theta, m_s)$  space that we should mention. In principle, the energy loss into sterile neutrinos produced in core collapse supernovae explosions provides bounds on the mass and mixing angles of massive (mostly sterile) neutrinos. However, so much is not understood about the neutrino transport and flavor transformation in hot and dense nuclear matter, that conservatively the implicated  $m_s - \sin^2 2\theta$  region can only be considered disfavored but not excluded. Only neutrinos with mass  $m_s \lesssim 150$  MeV could be emitted copiously in the supernova core and, for those masses, mixings  $\sin^2 2\theta_{\text{lim}} \equiv 3 \times 10^{-10} \lesssim \sin^2 2\theta \lesssim 10^{-2}$  are disfavored [18, 36]. For small mixing angles the sterile neutrinos are not trapped within the supernova, thus they are emitted from the whole collapsing star, mostly from its core. The lower bound on the mixing angle is obtained by requiring that the sterile neutrino flux at Earth emitted by the supernova 1987A,  $F_s$ , is not larger than the active flux,  $F_a = 1.1 \times 10^{10} \text{cm}^{-2}$ , emitted by it. Thus,  $F_s = F_a$  for  $\sin^2 2\theta_{\text{lim}}$  and for smaller angles

$$F_s = \frac{\sin^2 2\theta}{\sin^2 2\theta_{\text{lim}}} F_a. \quad (4.12)$$

This is relevant for the the last bound we will consider. The decay of heavy neutrinos emitted in supernova explosions would produce a flux of photons. The non-observation by the Solar Maximum Mission of any  $\gamma$ -ray counts in excess of the background for a time interval of  $t_{\text{max}} = 223.2$  sec after the arrival of the first  $\bar{\nu}_e$ 's from supernova 1987A, allows us to enlarge the disfavored regions of the parameter space. Following the analysis of Ref. [37] and neglecting the absorption of the photons produced in decays within the supernova, the  $\gamma$  flux is given by

$$\frac{dF_\gamma}{dE_\gamma} = \frac{F_s E_\gamma f_\gamma B}{T m_s \tau} \int_0^{t_{\text{max}}} dt e^{-2E_\gamma t/m_s \tau} \left(1 + \frac{E_\gamma}{T}\right) e^{-E_\gamma/T}. \quad (4.13)$$

Here  $T \simeq 50$  MeV is the temperature at which sterile neutrinos are emitted from the supernova core. We use the  $3\text{-}\sigma$  limits  $(\Delta F_\gamma)_{3\text{-}\sigma}(E_i, E_f)$  on the  $\gamma$  flux for the time interval considered obtained in Ref. [37] for three energy bands  $(E_i, E_f)$ , namely (4.1, 4.4) MeV, (10, 25) MeV and (25, 100) MeV (see Table 1 of Ref. [37]). We calculate the disfavored region in the  $(\sin^2 2\theta, m_s)$  parameter space by requiring

$$\int_{E_i}^{E_f} \frac{dF_\gamma}{dE_\gamma} dE_\gamma < (\Delta F_\gamma)_{3\text{-}\sigma}(E_i, E_f). \quad (4.14)$$

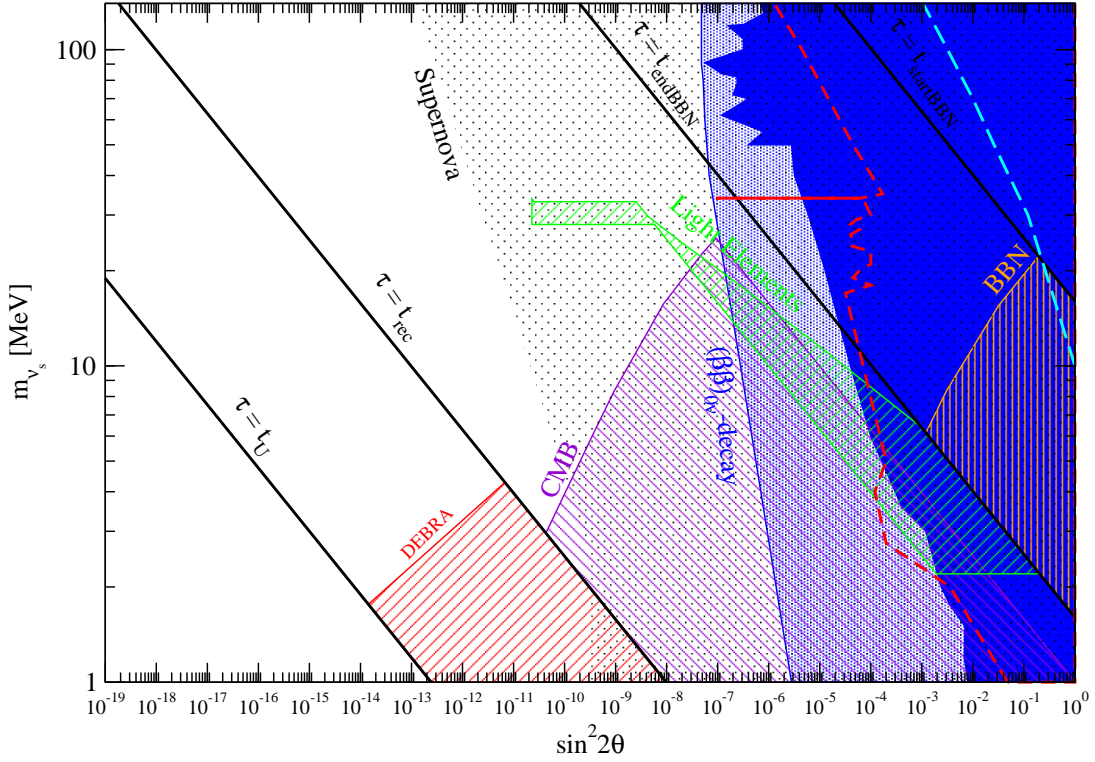


FIG. 7: Same as Fig. 4 but for a fixed value of the reheating temperature,  $T_{RH} = 5$  MeV and for heavy neutrino masses higher than 1 MeV.

In the limit  $m_s \tau \gg 2 t_{\max} T$ , which holds in the region of interest, this condition can be written as

$$\frac{F_s f_\gamma B}{2} \frac{2 t_{\max} T}{m_s \tau} G(E_i, E_f) < (\Delta F_\gamma)_{3-\sigma}(E_i, E_f), \quad (4.15)$$

with

$$G(E_i, E_f) \equiv 3 \left( e^{-E_i/T} - e^{-E_f/T} \right) + 3 \left( \left( \frac{E_i}{T} \right) e^{-E_i/T} - \left( \frac{E_f}{T} \right) e^{-E_f/T} \right) + \left( \left( \frac{E_i}{T} \right)^2 e^{-E_i/T} - \left( \frac{E_f}{T} \right)^2 e^{-E_f/T} \right). \quad (4.16)$$

The band which gives the most restrictive limits for the range of sterile neutrino masses considered is (25, 100) MeV, although the band (10, 25) MeV gives comparable results. The two types of regions disfavored by core collapse supernovae arguments are the dotted regions labeled “Supernova” in Figs. 4, 5, 6 and 7.

Figs. 4 to 7 show in the  $(\sin^2 2\theta, m_s)$  parameter space all the bounds on active-sterile neutrino mixing we have presented above, for  $T_{RH} > 4$  MeV and  $1 \text{ MeV} < m_s < 140$  MeV. For concreteness, in all the figures we have taken  $f_\gamma = 1$  and  $B = 0.1$ . Each cosmological bound is indicated by its corresponding label, as explained above. The regions globally excluded by laboratory measurements (Section III) are: the dark gray (blue) area for  $\nu_e - \nu_s$  mixing, the region to the right of the red short-dashed line for  $\nu_\mu - \nu_s$  mixing and that to the right of the (magenta) long-dashed line for  $\nu_\tau - \nu_s$  mixing. In the case of  $\nu_e - \nu_s$  mixing the bounds for Majorana neutrinos are more restrictive than for Dirac neutrinos (see the hatched dark gray (blue) area labeled as “ $(\beta\beta)_{0\nu}$ -decay”). Values of the heavy neutrino lifetime  $\tau$  equal to the relevant epochs in the history of the Universe are also shown.

In Figs. 4, 5 and 6, we display the results for three different values of the ratio  $x_{RH} \equiv m_s/T_{RH}$ ,  $x_{RH} = 1, 3, 10$ , respectively. As expected, for  $T_{RH}$  increasingly smaller than the sterile neutrino mass, the cosmological bounds become less restrictive, and when  $T_{RH} \leq m_s/10$ , the cosmological bounds become completely irrelevant and only experimental data are able to restrict the parameter space. This result can also be seen in Fig. 7, in which the reheating temperature is fixed to be  $T_{RH} = 5$  MeV. In this case all cosmological bounds become irrelevant for  $m_s \geq 30$  MeV.

## V. CONCLUSIONS

Sterile neutrinos are invoked in many extensions of the Standard Model of particle physics [13, 38, 39, 40]. However, it is commonly assumed that the cosmological and astrophysical bounds on the mixings of sterile and active neutrinos restrict the range of their allowed values much more than laboratory data. In fact, sterile neutrinos with parameters suitable to be found in the near future in different experiments would have mixings with active neutrinos too large to be allowed by the standard cosmological assumptions about the pre-BBN era in the Universe, an era about which we do not have any observational information. The standard assumptions are few but very powerful: it is usually assumed that the temperature reached in the radiation dominated epoch before BBN was very high, that the Universe was radiation dominated then and that the entropy of radiation and matter is conserved.

Here, we show that it is possible to evade most of the cosmological bounds by assuming that the temperature at the end of (the last episode of) inflation or entropy production, the so-called reheating temperature  $T_{\text{RH}}$ , is low enough. We concentrate on massive (mostly sterile) neutrinos heavier than 1 MeV, having previously dealt with the lighter ones [9]. For low  $T_{\text{RH}}$ , the production of sterile neutrinos is suppressed as shown in Fig. 1. For example, going from  $T_{\text{RH}} = m_s$  to  $T_{\text{RH}} = m_s/10$  there is a suppression of four orders of magnitude. We present the experimental bounds on sterile neutrino mixings and the cosmological bounds imposed by the diffuse extragalactic background radiation, the CMB, BBN and the abundance of light elements. We find that for  $T_{\text{RH}}$  a few times smaller  $m_s$  the cosmological bounds weaken significantly and for  $T_{\text{RH}} = m_s/10$  they disappear completely. This is shown in Figs. 4, 5, 6. In Fig. 7 we keep instead the reheating temperature at a fixed value  $T_{\text{RH}} = 5$  MeV, close to the lower bound on  $T_{\text{RH}}$  of 4 MeV imposed by BBN and other cosmological data. In this case, no cosmological bounds remain for  $m_s > 30$  MeV, thus the only constraints on sterile neutrinos in this mass range come from terrestrial experiments. Hence, unlike in the standard cosmology, in low reheating temperature cosmologies it is possible to accommodate “visible” sterile neutrinos, i.e., sterile neutrinos which could soon be found in experiments.

Cosmological scenarios with a very low reheating temperature are more complicated than the standard one. Although no consistent all-encompassing model of this nature exists at present, different aspects have been studied with interesting results, which suggest that a coherent scenario could be produced if an experimental indication would lead us to it. In fact, finding a particle, such as a “visible” sterile neutrino, whose existence would contradict the usual assumptions about the pre-BBN era, would give us not only invaluable information for particle physics, but also an indication of enormous relevance in cosmology: it would tell us that the usual assumptions must be modified, for example in the manner presented in this paper.

### Acknowledgments

SPR and SP thank UCLA for hospitality at the initial stages of this work. SP also thanks CERN for hospitality. GG was supported in part by NASA grants US DOE grant DE-FG03-91ER40662 Task C, and NASA grants NAG5-13399 and ATP03-0000-0057. SPR is partially supported by the Spanish Grant FPA2005-01678 of the MCT.

### Appendix

To be formally accurate, the derivation of Eq. (2.2) should be carried out in the mass basis, since the distribution function is defined for species of definite energy. In the vacuum limit, in which we are interested, one can start with the Boltzmann equation in terms of the 2 by 2 density matrix  $\rho$  acting on the mass eigenstates  $\nu_1$  and  $\nu_2$ , with elements  $\rho_{11}, \rho_{12}, \rho_{21}, \rho_{22}$  [41],

$$i\dot{\rho} = -[H, \rho] - i\{\Gamma, (\rho - \rho_{eq})\}, \quad (5.1)$$

where  $\rho_{eq}$  is given in terms of the equilibrium momentum distributions  $f_i^{\text{eq}}$  for  $i = 1, 2$ ,  $f_i^{\text{eq}} = (e^{(E_i - \mu_i)/T} + 1)^{-1}$  ( $E_i$  and  $\mu_i$  are the energy and chemical potential of the  $i$  mass eigenstate and without a lepton asymmetry  $\mu_i = 0$ ),

$$\rho_{eq} = \begin{bmatrix} f_1^{\text{eq}} & 0 \\ 0 & f_2^{\text{eq}} \end{bmatrix}, \quad (5.2)$$

and the 2 by 2 matrix  $H$  is

$$H = \begin{bmatrix} E_1 & 0 \\ 0 & E_2 \end{bmatrix}. \quad (5.3)$$

Neutrino production and destruction are represented by the anticommutator term in Eq. (5.1), which describes the coherence-breaking interactions. The matrix  $\Gamma$  can be written as

$$\Gamma = \begin{bmatrix} \cos^2 \theta(\Gamma/2 + \delta\Gamma_1) & -\cos \theta \sin \theta(\Gamma/2 + \delta\Gamma) \\ -\cos \theta \sin \theta(\Gamma/2 + \delta\Gamma) & \sin^2 \theta(\Gamma/2 + \delta\Gamma_2) \end{bmatrix}, \quad (5.4)$$

where  $\Gamma$  is the interaction rate for massless neutrinos, which is of order  $G_F^2$  (i.e., second order in the Fermi coupling constant),  $\delta\Gamma_i$  are the corrections necessary when the incoming and outgoing particles have a non-zero mass  $m_i$  in the case of scattering, or when the two annihilating particles are of mass  $m_i$  and  $\delta\Gamma$  is the correction necessary when one of the two interacting particles has mass  $m_1$  and the other has mass  $m_2$ .

Replacing Eqs. (5.2), (5.3) and (5.4) in Eq. (5.1) we can find the equation for  $\rho_{11}$ ,  $\rho_{22}$ , and  $\rho_{12}$ , which is the complex conjugate of  $\rho_{21}$ . Writing  $i\rho_{12} = R + iI$  and  $i\rho_{21} = R - iI$ , one can find the equations for the time derivative of the real and imaginary parts  $\dot{R}$  and  $\dot{I}$  in terms of  $R$  and  $I$ . As demonstrated in Ref. [42], in the stationary point or static approximation, we can take  $\dot{R} = \dot{I} = 0$  which allows us to solve for  $R$  and  $I$ . Using the expression for  $R$  and  $I$  so obtained and assuming that the less massive eigenstate  $\nu_1$  maintains equilibrium, for small values of  $\sin^2 2\theta$  one gets an expression for  $\rho_{22}$  which coincides with Eq. (2.2) in vacuum (once we take  $\rho_{22} = f_2 \simeq f_s$  and  $f_2^{\text{eq}} \simeq f_s^{\text{eq}}$ ).

- 
- [1] T. Moroi and L. Randall, Nucl. Phys. **B570**, 455 (2000) [arXiv:hep-ph/9906527].
- [2] M. Fujii and K. Hamaguchi, Phys. Rev. D **66**, 083501 (2002) [arXiv:hep-ph/0205044]; M. Fujii and M. Ibe, Phys. Rev. D **69**, 035006 (2004) [arXiv:hep-ph/0309064].
- [3] D. H. Lyth and E. D. Stewart, Phys. Rev. D **53**, 1784 (1996) [arXiv:hep-ph/9510204].
- [4] S. Hannestad, Phys. Rev. D **70**, 043506 (2004) [arXiv:astro-ph/0403291].
- [5] K. Ichikawa, M. Kawasaki and F. Takahashi, Phys. Rev. D **72**, 043522 (2005) [arXiv:astro-ph/0505395].
- [6] M. Kawasaki, K. Kohri and N. Sugiyama, Phys. Rev. Lett. **82**, 4168 (1999) [arXiv:astro-ph/9811437]; and Phys. Rev. D **62**, 023506 (2000) [arXiv:astro-ph/0002127].
- [7] G. F. Giudice, E. W. Kolb and A. Riotto, Phys. Rev. D **64**, 023508 (2001) [arXiv:hep-ph/0005123].
- [8] G. F. Giudice, E. W. Kolb, A. Riotto, D. V. Semikoz and I. I. Tkachev, Phys. Rev. D **64**, 043512 (2001) [arXiv:hep-ph/0012317].
- [9] G. Gelmini, S. Palomares-Ruiz and S. Pascoli, Phys. Rev. Lett. **93**, 081302 (2004) [arXiv:astro-ph/0403323]; G. B. Gelmini, Int. J. Mod. Phys. A **20**, 4670 (2005) [arXiv:hep-ph/0412304].
- [10] C. E. Yaguna, JHEP **0706**, 002 (2007) [arXiv:0706.0178 [hep-ph]].
- [11] A. D. Dolgov, K. Kohri, O. Seto and J. Yokoyama, Phys. Rev. D **67**, 103515 (2003) [arXiv:hep-ph/0210223].
- [12] G. B. Gelmini and P. Gondolo, Phys. Rev. D **74**, 023510 (2006) [arXiv:hep-ph/0602230]; G. Gelmini, P. Gondolo, A. Soldatenko and C. E. Yaguna, Phys. Rev. D **74**, 083514 (2006) [arXiv:hep-ph/0605016].
- [13] C. Boehm and P. Fayet, Nucl. Phys. B **683**, 219 (2004) [arXiv:hep-ph/0305261]; C. Boehm, Y. Farzan, T. Hambye, S. Palomares-Ruiz and S. Pascoli, Phys. Rev. D **77**, 043516 (2008) [arXiv:hep-ph/0612228].
- [14] S. Palomares-Ruiz and S. Pascoli, Phys. Rev. D **77**, 025025 (2008) [arXiv:0710.5420 [astro-ph]].
- [15] R. Barbieri and A. Dolgov, Phys. Lett. **B237**, 440 (1990); and Nucl. Phys. **B349**, 742 (1991); K. Enqvist, K. Kainulainen and J. Maalampi, Phys. Lett. **B244**, 186 (1990); and Phys. Lett. **B249**, 531 (1990).
- [16] S. Dodelson and L. M. Widrow, Phys. Rev. Lett. **72**, 17 (1994) [arXiv:hep-ph/9303287].
- [17] A. D. Dolgov and S. H. Hansen, Astropart. Phys. **16**, 339 (2002) [arXiv:hep-ph/0009083].
- [18] K. Abazajian, G. M. Fuller and M. Patel, Phys. Rev. D **64**, 023501 (2001) [arXiv:astro-ph/0101524].
- [19] A. D. Dolgov, S. H. Hansen, G. Raffelt and D. V. Semikoz, Nucl. Phys. B **590**, 562 (2000) [arXiv:hep-ph/0008138].
- [20] A. D. Dolgov, S. H. Hansen, G. Raffelt and D. V. Semikoz, Nucl. Phys. B **580**, 331 (2000) [arXiv:hep-ph/0002223].
- [21] S. H. Hansen and Z. Haiman, Astrophys. J. **600**, 26 (2004) [arXiv:astro-ph/0305126].
- [22] A. Atre, T. Han, S. Pascoli and B. Zhang, in preparation.
- [23] D. I. Britton *et al.*, Phys. Rev. Lett. **68**, 3000 (1992); D. I. Britton *et al.*, Phys. Rev. D **46**, 885 (1992).
- [24] H. O. Back *et al.*, JETP Lett. **78**, 261 (2003) [Pisma Zh. Eksp. Teor. Fiz. **78**, 707 (2003)]; C. Hagner *et al.*, Phys. Rev. D **52**, 1343 (1995).
- [25] G. Bernardi *et al.*, Phys. Lett. B **203**, 332 (1988).
- [26] A. Kusenko, S. Pascoli and D. Semikoz, JHEP **0511**, 028 (2005) [arXiv:hep-ph/0405198].
- [27] M. Daum *et al.*, Phys. Rev. Lett. **85** (2000) 1815 [arXiv:hep-ex/0008014].
- [28] R. S. Hayano *et al.*, Phys. Rev. Lett. **49** (1982) 1305.
- [29] E. Armengaud, G. Sigl, T. Beau and F. Miniati, Astropart. Phys. **28**, 463 (2007) [arXiv:astro-ph/0603675].
- [30] R. J. Protheroe and P. A. Johnson, Astropart. Phys. **4**, 253 (1996) [arXiv:astro-ph/9506119].
- [31] P. Sreekumar *et al.* [EGRET Collaboration], Astrophys. J. **494**, 523 (1998) [arXiv:astro-ph/9709257]; A. W. Strong, I. V. Moskalenko and O. Reimer, Astrophys. J. **613**, 956 (2004) [arXiv:astro-ph/0405441].
- [32] S. C. Kappadath *et al.*, Astron. Astrophys. **120**, 619 (1996); G. Weidespointner *et al.*, AIP Conf. Proc. **510**, 467 (2000).
- [33] J. R. Ellis, G. B. Gelmini, J. L. Lopez, D. V. Nanopoulos and S. Sarkar, Nucl. Phys. B **373**, 399 (1992).

- [34] W. Hu and J. Silk, Phys. Rev. Lett. **70** (1993) 2661.
- [35] D. J. Fixsen *et al.*, Astrophys. J. **473**, 576 (1996) [arXiv:astro-ph/9605054].
- [36] K. Kainulainen, J. Maalampi and J. T. Peltoniemi, Nucl. Phys. B **358** (1991) 435.
- [37] L. Oberauer, C. Hagner, G. Raffelt and E. Rieger, Astropart. Phys. **1**, 377 (1993).
- [38] T. Asaka, S. Blanchet and M. Shaposhnikov, Phys. Lett. B **631**, 151 (2005) [arXiv:hep-ph/0503065]; T. Asaka and M. Shaposhnikov, Phys. Lett. B **620**, 17 (2005) [arXiv:hep-ph/0505013].
- [39] A. de Gouvea, J. Jenkins and N. Vasudevan, Phys. Rev. D **75**, 013003 (2007) [arXiv:hep-ph/0608147]; A. de Gouvea, arXiv:0706.1732 [hep-ph].
- [40] T. Appelquist and R. Shrock, Phys. Rev. Lett. **90**, 201801 (2003) [arXiv:hep-ph/0301108]; Phys. Lett. B **548**, 204 (2002) [arXiv:hep-ph/0204141]; in Neutrino Factories and Superbeams, NuFact03, A.I.P. Conf. Proc, 721 (A.I.P., New York, 2004), p. 261; T. Appelquist, M. Piai and R. Shrock, Phys. Rev. D **69**, 015002 (2004) [arXiv:hep-ph/0308061]; T. Appelquist, N. D. Christensen, M. Piai and R. Shrock, Phys. Rev. D **70**, 093010 (2004) [arXiv:hep-ph/0409035].
- [41] A. D. Dolgov, Phys. Rept. **370**, 333 (2002) [arXiv:hep-ph/0202122].
- [42] N. F. Bell, R. R. Volkas and Y. Y. Y. Wong, Phys. Rev. D **59**, 113001 (1999) [arXiv:hep-ph/9809363].